

Article

Role of Cl on Diffusion of Cu in In₂S₃ Layers Prepared by Ion Layer Gas Reaction Method

Henry Wafula ^{1,*}, Musembi Robinson ², Albert Juma ³, Thomas Sakwa ¹, Manasse Kitui ¹, Rodrigo Araoz ³ and Christian-H. Fischer ³

¹ Physics Department, Masinde Muliro University of Science and Technology, Kakamega-50100, Kenya; E-Mails: tsakwa@mmust.ac.ke (T.S.); manassekitui2009@gmail.com (M.K.)

² Department of Physics, University of Nairobi, Nairobi-30197, Kenya; E-Mail: musembirj@uonbi.co.ke

³ Helmholtz-Zentrum Berlin für Materialien und Energie GmbH, Hahn-Meitner-Platz 1, 14109 Berlin, Germany; E-Mails: albert.juma@helmholtz-berlin.de (A.J.); rodrigo.saez@helmholtz-berlin.de (R.A.); fischer@helmholtz-berlin.de (C.-H.F.)

* Author to whom correspondence should be addressed; E-Mail: hbarasa@mmust.ac.ke; Tel.: +254-722-282-848.

Academic Editor: Alessandro Lavacchi

Received: 27 December 2014 / Accepted: 11 February 2015 / Published: 16 February 2015

Abstract: Ion layer gas reaction (ILGAR) method allows for deposition of Cl-containing and Cl-free In₂S₃ layers from InCl₃ and In(OCCH₃CHOCCH₃)₃ precursor salts, respectively. A comparative study was performed to investigate the role of Cl on the diffusion of Cu from CuSCN source layer into ILGAR deposited In₂S₃ layers. The Cl concentration was varied between 7 and 14 at.% by varying deposition parameters. The activation energies and exponential pre-factors for Cu diffusion in Cl-containing samples were between 0.70 to 0.78 eV and between 6.0×10^{-6} and 3.2×10^{-5} cm²/s. The activation energy in Cl-free ILGAR In₂S₃ layers was about three times less compared to the Cl-containing In₂S₃, and the pre-exponential constant six orders of magnitude lower. These values were comparable to those obtained from thermally evaporated In₂S₃ layers. The residual Cl-occupies S sites in the In₂S₃ structure leading to non-stoichiometry and hence different diffusion mechanism for Cu compared to stoichiometric Cl-free layers.

Keywords: diffusion; ILGAR; In₂S₃; CuSCN

1. Introduction

In₂S₃ has found increased attention in photovoltaic's as a replacement for toxic CdS [1–4] because of its suitable properties. It has been effectively used as a buffer layer for both chalcopyrite [1–3] and nanocomposites [5,6] solar cells and as an extremely thin absorber (eta) in eta cells [7,8] and nanocomposites [9] solar cells with ZnO nanorods or nanoporous-TiO₂ electrodes, respectively. Diffusion of Cu from Cu(In,Ga)(S,Se)₂ absorber [3,10,11] or CuSCN hole conductor [12] into In₂S₃ layers has been a major drawback to effective performance and stability of these solar cells.

In₂S₃ exists in three phases: β -phase which is stable at room temperature up to 420° [13,14], the α -phase which is stable above 420 °C [15] up to 754 °C and the γ -phase which is stable between 754 °C and its melting point 1090 °C [16]. The most commonly used phase is the β -In₂S₃. β -In₂S₃ has a defect spinel superstructure in which In occupies all octahedral sites and a third of the tetrahedral sites [16,17]. A third of the tetrahedral cationic sites remain vacant but ordered along 4₁ screw with alignment of three spinel blocks in c-direction [17]. β -In₂S₃ can accommodate foreign atoms, for example Fe [18], Ag [19], Cl [20], Cu and Na [10].

The presence of foreign impurities in host In₂S₃ affects occupation and migration of new foreign atoms. Diffusion of Cu in In₂S₃ is inhibited by the presence of Na because both Na and Cu compete for the same cationic vacancies and substitution sites in In₂S₃ structure [21]. Different authors have reported diffusion of Cu in In₂S₃ to be governed by vacancy [22] or insertion/substitution [21] mechanism. A better understanding and hence control of Cu diffusion in In₂S₃ layers is crucial for photovoltaic applications [23].

ILGAR is a sequential and cyclic method of depositing highly conformal In₂S₃ layers on different substrates [24,25]. In₂S₃ layers can be deposited from InCl₃ or In(OCCH₃CHOCC₃)₃ to obtain Cl-free and Cl-containing layers [26]. The presence of Cl in In₂S₃ increased the optical band up to 2.4 eV compared to 2.0 eV for Cl-free layers. Higher conversion efficiency was achieved for Cl-free In₂S₃ layers compared to Cl-containing layers both prepared by ILGAR [26]. The stoichiometry as well as opto-electronic properties of In₂S₃ layers also changes with inclusion of Cl. Crystallinity and photosensitivity increased with increasing Cl content [20]. It is therefore important to investigate the effect of Cl on diffusion of Cu in ILGAR deposited In₂S₃ layers.

Rutherford backscattering spectroscopy (RBS) is an absolute method for determination of elemental composition and depth profiling of various materials with high accuracy [27,28]. The diffusion coefficient of Cu in In₂S₃ can be obtained from Cu concentration profiles by solving the diffusion equation analytically or numerically with appropriate boundary conditions and comparing or fitting the resulting profiles with the experimental data. Activation energy and diffusion prefactor of 0.3 eV and $9 \times 10^{-11} \text{ cm}^2 \cdot \text{s}^{-1}$ determined from RBS depth profiling have been reported for Cu diffusion in thermally evaporated In₂S₃ layers [23].

In this work, we report a comparative study of Cu diffusion in Cl-free and Cl-containing In₂S₃ layers. In₂S₃ layers were prepared by ILGAR method, which was modified to obtain layers with varying Cl content. The Cu source was CuSCN deposited on top of In₂S₃. The distribution of diffused Cu in In₂S₃ was profiled by RBS from which the diffusion coefficients were determined as a function of annealing temperature.

2. Experimental Section

In₂S₃ layers were deposited by ILGAR [24,25] onto c-Si wafers without additional treatment of the c-Si substrates. InCl₃ or In(acac)₃ precursor salt was dissolved into ethanol solvent to obtain a solution of 25 mM. In(acac)₃ precursor was used to deposit Cl-free layers while InCl₃ was used for Cl-containing layers. The deposition temperature for deposition of all samples was 200 °C. The standard ILGAR cycles were adjusted to produce In₂S₃ layers with varying Cl content. The details of the deposition parameters for the different samples are given in Table 1. CuSCN was deposited onto each of the c-Si/In₂S₃ samples by spray-spin coating method [23] from a solution of 50 mM CuSCN dissolved in propyl sulfide [29]. For each sample, ten spray-spin coating cycles were deposited, which corresponds to about 500 nm thickness as determined by Dektak profilometer before heat treatment, while the thickness of the samples after heat treatment varied as shown in Table 1. The c-Si/In₂S₃/CuSCN samples were then cut into smaller sizes of about 7 mm × 7 mm. The smaller pieces were then annealed for 5 min at temperatures between 150 °C and 250 °C. A set of small samples annealed at these temperatures and one not annealed was obtained for each large c-Si/In₂S₃/CuSCN sample.

CuSCN layer was then etched away in pyridine solution [23]. The sample was first dipped into pyridine solution for 2 s then rinsed in deionized water to wash away the pyridine. This was repeated until a shiny surface similar to the as-deposited In₂S₃ was obtained. RBS measurements were performed with 1.4 MeV He⁺ ion beam and the backscattered ions detected at a scattering angle of 168° [23].

3. Results and Discussion

The composition of In₂S₃(acac) and In₂S₃(Cl) was determined from RBS measurements on as-deposited samples. The integral of the respective peaks were used to calculate the areal densities, from which the layer thicknesses were obtained. The number of atoms ($N_i t$) of a given element in a layer is given by [27],

$$N_i t = \frac{A \cos \theta_1}{Q \Omega \sigma(E_0)} \quad (1)$$

where t is the layer thickness, A the integral of the peak, Q the number of ions incident on the sample, Ω the detector solid angle and $\sigma(E_0)$ the differential scattering cross-section. The concentration of each element was obtained by dividing the atomic density (N_i) of each element by that of In₂S₃ ($4.53 \times 10^{22} \text{ cm}^{-3}$). The values of the atomic concentrations and layer thicknesses of the samples are given in Table 1.

Table 1. Thickness and layer composition of In₂S₃ films.

Name	Thickness (nm)	In (at.%)	S (at.%)	Cl (at.%)	S/In
S0	86	39	61	0	1.56
S8	152	37.5	52.2	11.3	1.41
S9	65	37.1	49.1	13.8	1.32
S11	64	37.8	54.4	7.8	1.44
S12	45	37.6	53.9	8.6	1.43

Sample S0 was $\text{In}_2\text{S}_3(\text{acac})$ while samples S8, S9, S11 and S12 were $\text{In}_2\text{S}_3(\text{Cl})$. Deposition parameters were adjusted to obtain $\text{In}_2\text{S}_3(\text{Cl})$ with different Cl content. The difference in layer thicknesses was due to a difference in deposition rate due to the changes in the deposition steps. The presence of large amounts of Cl in $\text{In}_2\text{S}_3(\text{Cl})$ layers led to a strong deviation from stoichiometry while $\text{In}_2\text{S}_3(\text{acac})$ layers were more stoichiometric with S/In ratio of 1.56, which is very close to the expected value of 1.5. The amount of In was almost constant for all $\text{In}_2\text{S}_3(\text{Cl})$ samples while S content dependent on the residual Cl. This means that the InCl_3 precursor layers were not completely sulfurized, leaving behind Cl residues.

RBS spectra for $\text{In}_2\text{S}_3(\text{acac})$ and $\text{In}_2\text{S}_3(\text{Cl})$ containing diffused Cu after annealing for 5 min at different temperatures are shown in Figure 1. The various peaks corresponding to the elements detected in the samples are shown. The Cu peak increases in height with increasing diffusion (annealing) temperature. The shape of the peaks depicts a concentration gradient of Cu in In_2S_3 with higher concentration at the surface. Inclusion of Cu into In_2S_3 matrix results in an increase in the volume of the In_2S_3 that can be seen by increase in the width of the In and S peaks with increasing diffusion temperature.

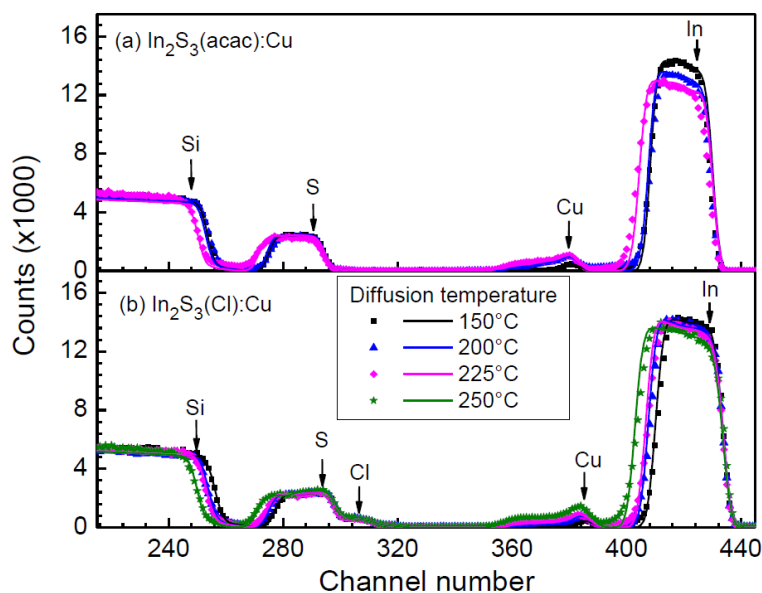


Figure 1. RBS spectra for (a) $\text{In}_2\text{S}_3(\text{acac})\text{:Cu}$ and (b) $\text{In}_2\text{S}_3(\text{Cl})\text{:Cu}$ after diffusion of Cu at different temperatures. The respective peaks are indicated.

Figure 2 shows the Cu peaks from Figure 1. The distribution of Cu in the In_2S_3 bulk is not similar for $\text{In}_2\text{S}_3(\text{acac})\text{:Cu}$ and $\text{In}_2\text{S}_3(\text{Cl})\text{:Cu}$ layers. The distribution in the other $\text{In}_2\text{S}_3(\text{Cl})\text{:Cu}$ layers with varying Cl content was similar to Figure 2b. The Cu peaks increased systematically with diffusion temperature for $\text{In}_2\text{S}_3(\text{acac})\text{:Cu}$ similar to the case for thermally evaporated In_2S_3 layers reported in reference [23].

The Cu peaks from $\text{In}_2\text{S}_3(\text{Cl})\text{:Cu}$ increased slowly with diffusing temperature for temperatures below 200 °C and then increased strongly above 200 °C. The distribution of Cu tends to be more constant in the $\text{In}_2\text{S}_3(\text{Cl})\text{:Cu}$ bulk than in $\text{In}_2\text{S}_3(\text{acac})\text{:Cu}$. The difference in the nature of the concentration gradients can be attributed to the presence of Cl. Cl therefore plays a crucial role in the diffusion of Cu in In_2S_3 layers.

The depth profiles of Cu were extracted from the Cu peaks of the RBS spectra for the different samples using WinDF software [30]. A recursion equation was developed from the Fick's second law of diffusion and used to numerically calculate the Cu concentration profiles and compare the results to

the measured data. Details can be found in reference [23]. The depth profiles were fitted numerically with minimum deviation and values for the diffusion coefficients were obtained. The measured and simulated depth profiles for $\text{In}_2\text{S}_3(\text{acac})\text{:Cu}$ and $\text{In}_2\text{S}_3(\text{Cl})\text{:Cu}$ are shown in Figure 3.

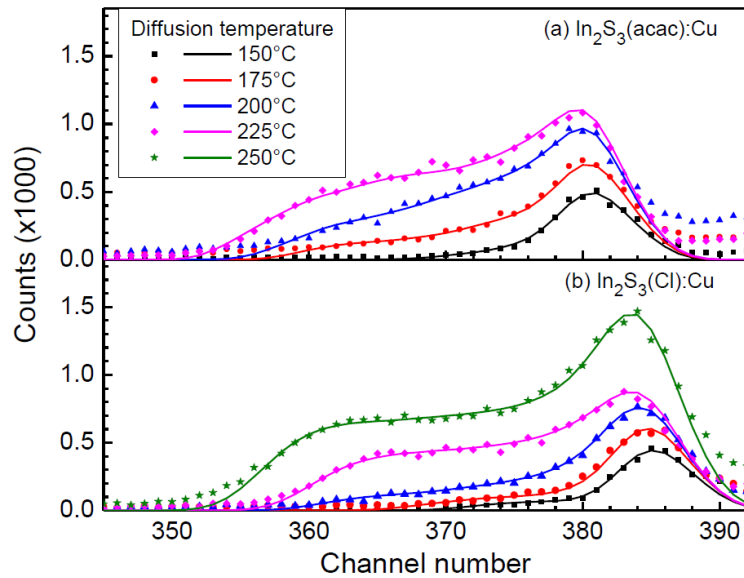


Figure 2. Cu peaks for (a) $\text{In}_2\text{S}_3(\text{acac})\text{:Cu}$ and (b) $\text{In}_2\text{S}_3(\text{Cl})\text{:Cu}$ for different diffusion temperatures. The scatters represent measured data while the solid lines are from simulation.

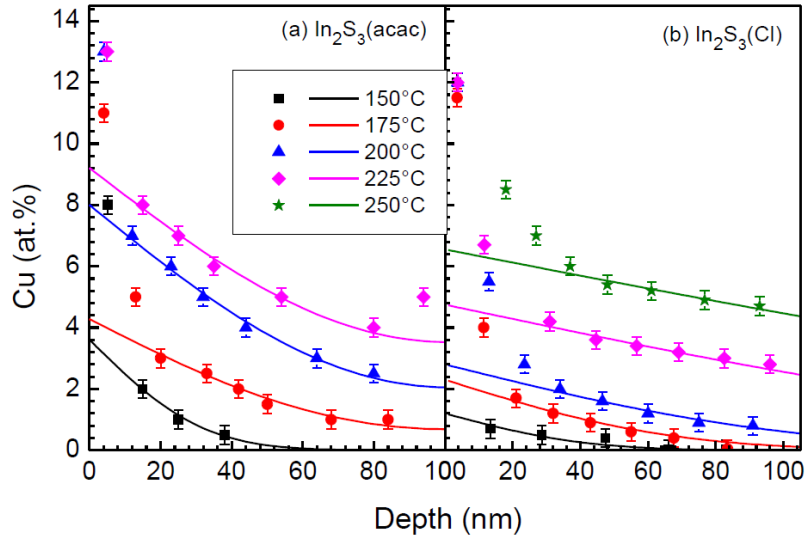


Figure 3. Simulated and measured depth profiles for Cu in (a) $\text{In}_2\text{S}_3(\text{acac})\text{:Cu}$ and (b) $\text{In}_2\text{S}_3(\text{Cl})\text{:Cu}$ from which diffusion coefficients were determined.

The depth profiles show a thin surface layer with high Cu concentration independent of diffusion temperature. This means an interfacial layer with a large amount of Cu was formed upon deposition of CuSCN and annealing. A thin interfacial layer due to diffusion of Cu into In_2S_3 layer was also observed for $\text{Cu}(\text{In,Ga})\text{Se}_2/\text{In}_2\text{S}_3$ layer system for Chalcopyrite solar cells [3]. This thin surface layer was therefore not used in fitting the profiles to obtain diffusion coefficient values.

Diffusion coefficient values were calculated for all the samples with different Cl contents and plotted against inverse temperature in an Arrhenius plot as shown in Figure 4. The activation energy of Cu diffusion in the different In₂S₃ layers and exponential prefactors were obtained from the Arrhenius plots. The results for Cu diffusion in thermally evaporated In₂S₃ layers [23] are included for comparison.

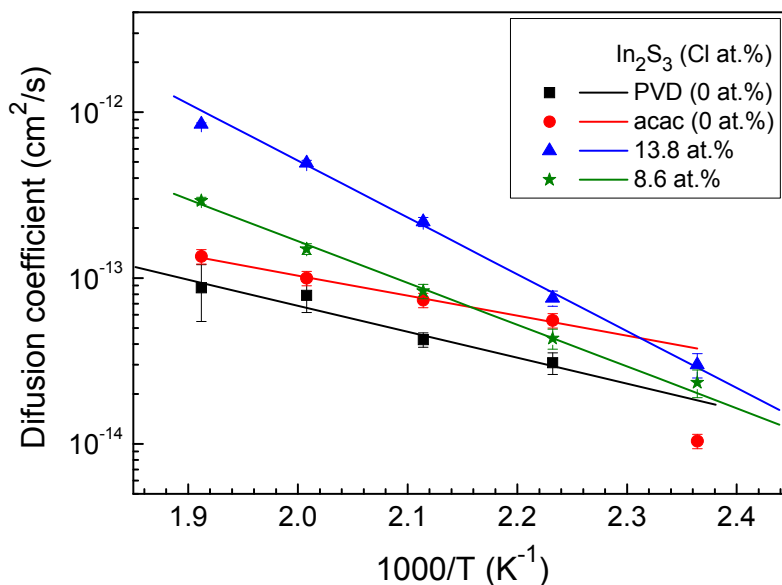


Figure 4. Arrhenius plot of diffusion coefficient against inverse temperature for different In₂S₃ layers.

The values of the activation energies and exponential prefactor for all the samples with different Cl concentrations are shown in Table 2.

Table 2. Activation energy and exponential prefactor of In₂S₃ films with varying chlorine percentages.

In ₂ S ₃ films	Activation energy E_A (eV)	Exponential prefactor D_0 (cm ² /s)
In ₂ S ₃ :Cl 13.8 at.%	0.70	6.0×10^{-6}
In ₂ S ₃ :Cl 11.3 at.%	0.72	3.0×10^{-6}
In ₂ S ₃ :Cl 8.5 at.%	0.78	3.2×10^{-5}
In ₂ S ₃ :Cl 7.8 at.%	0.76	1.2×10^{-5}
In ₂ S ₃ :acac	0.24	2.7×10^{-11}
In ₂ S ₃ :PVD	0.30	9.0×10^{-11}

The activation energy and prefactor for the diffusion of Cu in Cl-free In₂S₃ layers was of the same order for In₂S₃ deposited by ILGAR and PVD but much lower than in Cl-containing layers. Residual Cl in In₂S₃ is known to occupy S places in the In₂S₃ matrix resulting in an increase in the optical band gap, photosensitivity and a decrease in work function [4,20,31]. The presence of Cl changes the stoichiometry and local bond configuration of In₂S₃ and this can limit Cu migration in In₂S₃:Cl compared to migration in stoichiometric In₂S₃. The In–Cl bond energy is much stronger than that of In–S and this could be the reason for the higher activation energy needed for Cu to diffuse in Cl-containing In₂S₃. A higher amount of energy is therefore required to overcome the barrier for Cu migration. The prefactor in In₂S₃:Cl was five to six orders of magnitude higher than in In₂S₃:acac and In₂S₃:PVD. An increase in the prefactor could be concomitant with an increase in the entropy.

4. Conclusions

In₂S₃ layers were deposited by Ion layer gas reaction onto c-Si wafers and CuSCN deposited onto the samples by spray-spin coating, deposition parameters were varied to obtain varying chlorine contents in the sample that ranged from 7.8 at.% to 13.8 at.%. The distribution of copper in the samples with chlorine was strongly influenced by chlorine for annealing temperatures above 200 °C. This shows that chlorine plays a crucial role in copper diffusion in In₂S₃. The activation energies and exponential prefactors for Cu diffusion in Chlorine containing samples were between 0.7 to 0.78 eV and between 6×10^{-6} and 3.2×10^{-5} cm²/s. The activation energy in Cl free In₂S₃ layers was about three times less and the pre-exponential constant six orders of magnitude lower.

Acknowledgments

The authors of this paper would like to thank Helmholtz-Zentrum Berlin for the experimentation, Friedrich Schiller University Physics Department, Jena for RBS analysis and Deutscher Akademischer Austausch Dienst (DAAD) for financial support.

Author Contributions

Henry Wafula and Albert Juma designed and performed the experiments, prepared the manuscript. Robinson Musembi, Thomas Sakwa, Manasse Kitui, Rodrigo Saez and Christian-Herbert Fischer performed expert analysis of the results.

Conflicts of Interest

The authors declare no conflict of interest.

References

1. Barreau, N.; Bernéde, J.C.; El Maliki, H.; Marsillac, S.; Castel, X.; Pinel, J. Recent studies on In₂S₃ containing oxygen thin films. *Solid State Commun.* **2002**, *122*, 445–450.
2. Bär, M.; Allsop, N.; Lauer mann, I.; Fischer, C.-H. Deposition of In₂S₃ on Cu(In,Ga)(S,Se)₂ thin film solar cell absorbers by spray ion layer gas reaction: Evidence of strong interfacial diffusion. *Appl. Phys. Lett.* **2007**, *90*, doi:10.1063/1.2717534.
3. Abou-Ras, D.; Kostorz, G.; Strohm, A.; Schock, H.-W.; Tiwari, A.N. Interfacial layer formations between Cu(In, Ga)Se₂ and In_xS_y layers. *J. Appl. Phys.* **2005**, *98*, doi:10.1063/1.2149166.
4. Barreau, N. Indium sulfide and relatives in the world of photovoltaics. *Sol. Energy* **2009**, *83*, 363–371.
5. Nanu, M.; Schoonman, J.; Goossens, A. Nanocomposite three-dimensional solar cells obtained by chemical spray deposition. *Nano Lett.* **2005**, *5*, 1716–1719.
6. Nanu, M.; Schoonman, J.; Goossens, A. Inorganic nanocomposites of n- and p-type semiconductors: A new type of three-dimensional solar cell. *Adv. Mater.* **2004**, *16*, 453–456.

7. Belaidi, A.; Dittrich, T.; Kieven, D.; Tornow, J.; Schwarzburg, K.; Kunst, M.; Allsop, N.; Lux-Steiner, M.-C.; Gavrilov, S. ZnO-nanorod arrays for solar cells with extremely thin sulfidic absorber. *Sol. Energy Mater. Sol. Cells* **2009**, *93*, 1033–1036.
8. Kieven, D.; Dittrich, T.; Belaidi, A.; Tornow, J.; Schwarzburg, K.; Allsop, N.; Lux-Steiner, M. Effect of internal surface area on the performance of ZnO/In₂S₃/CuSCN solar cells with extremely thin absorber. *Appl. Phys. Lett.* **2008**, *92*, doi:10.1063/1.2909576.
9. Herzog, C.; Belaidi, A.; Ogacho, A.; Dittrich, T. Inorganic solid state solar cell with ultra-thin nanocomposite absorber based on nanoporous TiO₂ and In₂S₃. *Energy Environ. Sci.* **2009**, *2*, 962–964.
10. Abou-Ras, D.; Rudmann, D.; Kostorz, G.; Spiering, S.; Powalla, M.; Tiwari, A.N. Microstructural and chemical studies of interfaces between Cu(In,Ga)Se₂ and In₂S₃ layers. *J. Appl. Phys.* **2005**, *97*, doi:10.1063/1.1863454.
11. Pistor, P.; Allsop, N.; Braun, W.; Caballero, R.; Camus, C.; Fischer, C.-H.; Gorgoi, M.; Grimm, A.; Johnson, B.; Kropp, T.; *et al.* Cu in In₂S₃: Interdiffusion phenomena analysed by high kinetic energy X-ray photoelectron spectroscopy. *Phys. Status Solidi A* **2009**, *206*, 1059–1062.
12. Dittrich, T.; Kieven, D.; Belaidi, A.; Rusu, M.; Tornow, J.; Schwarzburg, K.; Lux-Steiner, M.C. Formation of the charge selective contact in solar cells with extremely thin absorber based on ZnO-nanorod/In₂S₃/CuSCN. *J. Appl. Phys.* **2009**, *105*, doi:10.1063/1.3077259.
13. Rooyman, C.J.M. A new type of cation-vacancy ordering in the spinel lattice of In₂S₃. *J. Inorg. Nucl. Chem.* **1959**, *11*, 78–79.
14. King, G.S.D. The space group of β-In₂S₃. *Acta Cryst.* **1962**, *15*, 512.
15. Hahn, H.; Klinger, W. The crystal structures of the In₂S₃ and In₂Te₃. *Z. Anorg. Chem.* **1949**, *260*, 97–109.
16. Diehl, R.; Carpentier, C.-D.; Nitsche, R. The crystal structure of γ-In₂S₃ stabilized by As or Sb. *Acta Cryst.* **1976**, *B32*, 1257–1260.
17. Diehl, R.; Nitsche, R. Vapour growth of three In₂S₃ modifications by iodine transport. *J. Cryst. Growth* **1975**, *28*, 306–310.
18. Womes, M.; Olivier-Fourcade, J.; Jumas, J.-C.; Aubertin, F.; Gonser, U. Characterization of the single phase region with spinel structure in the ternary system In₂S₃-FeS-FeS₂. *J. Solid State Chem.* **1992**, *97*, 249–256.
19. Mathew, M.; Sudha Kartha, C.; Vijayakumar, K.P. In₂S₃:Ag, an ideal buffer layer for thin film solar cells. *J. Mater. Sci. Mater. Electron.* **2009**, *20*, 294–298.
20. Cherian, A.S.; Mathew, M.; Kartha, C.S.; Vijayakumar, K.P. Role of chlorine on the opto-electronic properties of β-In₂S₃ thin films. *Thin Solid Films* **2010**, *518*, 1779–1783.
21. Guillot-Deudon, C.; Harel, S.; Mokrani, A.; Lafond, A.; Barreau, N.; Fernandez, V.; Kessler, J. Electronic structure of Na_xCu_{1-x}In₅S₈ compounds: X-ray photo emission spectroscopy study and band structure calculations. *Phys. Rev. B* **2008**, *78*, doi:10.1103/PhysRevB.78.235201.
22. Py, F.; Womes, M.; Durand, J.M.; Olivier-Fourcade, J.; Jumas, J.-C.; Esteva, J.M.; Karnatak, R.C. Copper in In₂S₃: A study by X-ray diffraction, diffuse reflectance and X-ray absorption. *J. Alloys Compd.* **1992**, *178*, 297–304.
23. Juma, A.O.; Pistor, P.; Fengler, S.; Dittrich, T.; Wendler, E. Copper diffusion in thin In₂S₃ layers investigated by Rutherford Backscattering spectroscopy. *Thin Solid Films* **2012**, *520*, 6740–6743.

24. Fischer, C.-H.; Muffler, H.-J.; Bär, M.; Fiechter, S.; Leupolt, B.; Lux-Steiner, M.C. Ion layer gas Reaction (ILGAR)-conversion thermodynamic considerations and related FTIR analysis. *J. Cryst. Growth* **2002**, *241*, 151–158.
25. Gledhill, S.; Allison, R.; Allsop, N.; Fu, Y.; Kanaki, E.; Sáez-Araoz, R.; Lux-Steiner, M.; Fischer, C.-H. The reaction mechanism of the spray ion layer Gas reaction process to deposit In_2S_3 thin films. *Thin Solid Films*. **2011**, *519*, 6413–6419.
26. Sáez-Araoz, R.; Krammer, J.; Harndt, S.; Koehler, T.; Krueger, M.; Pistor, P.; Jasenek, A.; Hergert, F.; Lux-Steiner, M.C.; Fischer, C.-H. ILGAR In_2S_3 buffer layers for Cd-free $\text{Cu}(\text{In,Ga})(\text{S,Se})_2$ solar cells with certified efficiencies above 16%. *Prog. Photovolt. Res. Appl.* **2012**, *20*, 855–861.
27. Jeynes, C.; Barradas, N.P.; Szilágyi, E. Accurate determination of quantity of material in thin films by rutherford backscattering spectrometry. *Anal. Chem.* **2012**, *84*, 6061–6069.
28. Jeynes, C.; Barradas, N.P.; Rafla-Yuan, H.; Hichwa, B.P.; Close, R. Accurate depth profiling of complex optical coatings. *Surf. Interface Anal.* **2000**, *30*, 237–242.
29. Kumara, G.R.R.A.; Konno, A.; Senadeera, G.K.R.; Jayaweera, P.V.V.; de Silva, D.B.R.A.; Tennakone, K. Dye-sensitized solar cell with the hole collector p-CuSCN deposited from a solution in-propyl Sulphide. *Sol. Energy Mater. Sol. Cells* **2001**, *69*, 195–199.
30. Barradas, N.P.; Jeynes, C.; Webb, R.P. Simulated annealing analysis of Rutherford backscattering data. *Appl. Phys. Lett.* **1997**, *71*, doi:10.1063/1.119524.
31. Juma, A.O.; Azarpira, A.; Steigert, A.; Pomaska, M.; Fischer, C.-H.; Lauermann, I.; Dittrich, T. Role of chlorine in In_2S_3 for band alignment at nanoporous- $\text{TiO}_2/\text{In}_2\text{S}_3$ Interfaces. *J. Appl. Phys.* **2013**, *114*, doi:10.1063/1.4817766.

© 2015 by the authors; licensee MDPI, Basel, Switzerland. This article is an open access article distributed under the terms and conditions of the Creative Commons Attribution license (<http://creativecommons.org/licenses/by/4.0/>).